Cardiac stem cells delivered intravascularly traverse the vessel barrier, regenerate infarcted myocardium, and improve cardiac function

Buddhadeb Dawn*, Adam B. Stein*, Konrad Urbanek†, Marcello Rota†, Brian Whang†, Raffaella Rastaldo†, Daniele Torella†, Xian-Liang Tang*, Arash Rezazadeh*, Jan Kajstura†, Annarosa Leri†, Greg Hunt*, Jai Varma*, Sumanth D. Prabhu*, Piero Anversa†, and Roberto Bolli*‡

*Institute of Molecular Cardiology, University of Louisville, Louisville, KY 40202; and †Cardiovascular Research Institute, Department of Medicine, New York Medical College, Valhalla, NY 10595

Edited by Eric N. Olson, University of Texas Southwestern Medical Center, Dallas, TX, and approved January 27, 2005 (received for review August 13, 2004)

The ability of cardiac stem cells (CSCs) to promote myocardial repair under clinically relevant conditions (i.e., when delivered intravascularly after reperfusion) is unknown. Thus, rats were subjected to a 90-min coronary occlusion; at 4 h after reperfusion, CSCs were delivered to the coronary arteries via a catheter positioned into the aortic root. Echocardiographic analysis showed that injection of CSCs attenuated the increase in left ventricular (LV) end-diastolic dimensions and impairment in LV systolic performance at 5 weeks after myocardial infarction. Pathologic analysis showed that treated hearts exhibited a smaller increase in LV chamber diameter and volume and a higher wall thickness-to-chamber radius ratio and LV mass-to-chamber volume ratio. CSCs induced myocardial regeneration, decreasing infarct size by 29%. A diploid DNA content and only two chromosomes 12 were found in new cardiomyocytes, indicating that cell fusion did not contribute to tissue reconstitution. In conclusion, intravascular injection of CSCs after reperfusion limits infarct size, attenuates LV remodeling, and ameliorates LV function. This study demonstrates that CSCs are effective when delivered in a clinically relevant manner, a clear prerequisite for clinical translation, and that these beneficial effects are independent of cell fusion. The results establish CSCs as candidates for cardiac regeneration and support an approach in which the heart's own stem cells could be collected, expanded, and stored for subsequent therapeutic repair.

myocardial infarction | myocardial regeneration

With the recent surge of interest in cardiac regenerative therapies for patients with acute myocardial infarction (MI) (1), the identification of clinically applicable strategies is of paramount importance. Several cell types have been used in an effort to reconstitute dead myocardium. Among them, endothelial progenitor cells and bone marrow-derived cells have been the most successful (2–6). However, preliminary long-term studies with bone marrow-derived cells indicate that the new myocytes do not acquire the adult phenotype but resemble neonatal cells, which die with time by apoptosis (P.A., unpublished data). Intense efforts continue to focus on identifying an effective cell population and an effective mode of delivery.

The discovery that the adult heart contains a pool of cardiac stem cells (CSCs) that can replenish the cardiomyocyte population and generate coronary vessels (7–12) has dramatically changed the traditional view of the heart as a postmitotic organ. Because of its natural role in regeneration of cardiac cells, the endogenous CSC appears to be the ideal cell for myocardial repair. Recent studies have shown that when c-kit^{POS} CSCs are injected directly into the myocardium adjacent to an infarct produced by a permanent coronary occlusion, they migrate to the infarct and reconstitute part of the dead tissue, reducing infarct size and ameliorating cardiac function in rats (9) and mice (12). In contrast, i.v. injection of CSCs in mice subjected to transient coronary occlusion results in a miniscule amount of regeneration (≈3% of total cardiac cells) (10) (in that study, cardiac function was not assessed). These investigations (9, 10, 12) suggest that CSCs have the potential to reconstitute dead myocardium, but a number of fundamental issues need to be addressed before this approach can be considered for translational studies. First, although the majority of patients with acute MI undergo spontaneous or iatrogenic reperfusion, the ability of CSCs to improve cardiac function in the setting of a reperfused infarction has never been tested. The literature is replete with examples of therapies that work in the presence of a transient but not permanent coronary occlusion (13). Consequently, it is of the utmost importance to determine whether CSCs are effective when the coronary occlusion is followed by reperfusion, an event that dramatically alters the milieu of the heart (14). Second, improvement in LV function has been shown when CSCs were injected intramyocardially in the periinfarct area (9), an approach that would be difficult in patients. Clinically, the most practical route for CSC administration is intravascular delivery, but it is unknown whether CSCs injected into the coronary circulation can cross the vessel wall, translocate to the infarcted region, and initiate effective myocardial regeneration. Finally, the mechanism whereby CSCs improve cardiac function (differentiation into cardiac cells vs. fusion vs. paracrine effects on preexisting cells) remains poorly understood.

The goal of this study is to address these issues with a thorough comprehensive investigation that includes large sample sizes, blinded analyses of data, and simultaneous assessment of cardiac structure and function. Specifically, we investigated whether a clinically relevant modality of CSC administration (i.e., intravascular delivery) is effective in reconstituting infarcted myocardium in a clinically relevant rat model (temporary coronary occlusion followed by reperfusion) designed to mimic the most common clinical condition in acute MI. We also performed a thorough analysis of possible cell fusion.

Materials and Methods

A detailed description of all materials and methods is provided in *Supporting Text*, which is published as supporting information on the PNAS web site.

Isolation and Culture of CSCs. CSCs were isolated from the ventricle of adult Fischer 344 rats. Clonogenic cells obtained by cell sorting and single cell cloning were infected with a retrovirus carrying EGFP (9).

This paper was submitted directly (Track II) to the PNAS office.

Abbreviations: CSC, cardiac stem cell; LV, left ventricular; MI, myocardial infarction.

‡To whom correspondence should be addressed. E-mail: rbolli@louisville.edu.

www.pnas.org/cgi/doi/10.1073/pnas.0405957102

Ischemia/Reperfusion Injury. Anesthetized female Fischer 344 rats (age 3–4 months) underwent an open-chest 90-min occlusion of the left anterior descending coronary artery followed by reperfusion. Four hours after reperfusion, 1×10^6 CSCs or vehicle were injected into the aortic root during two 20-s occlusions of the aorta and pulmonary artery. In sham-operated rats, the chest was opened, but no injection was done. Rats were killed 5 weeks later.

Echocardiography and Hemodynamics. Serial echocardiograms were obtained at baseline (2 days before coronary occlusion) and 2 and 35 days after reperfusion. Anatomical and functional parameters were calculated by using standard methods (15). The hemodynamic studies were performed at 35 days after surgery, just before death.

Morphometry and Histology. The heart was perfusion-fixed in formalin and embedded in paraffin. Using an image analyzer, morphometric parameters were obtained from serial LV sections (16). Immunohistochemistry was performed in formalin-fixed 4-μm-thick sections by using the antibodies specified in Table 1, which is published as supporting information on the PNAS web site (7–9).

Cell Volume of EGFP^{POS} and EGFP^{NEG} Myocytes. LV myocytes were enzymatically dissociated from CSC-treated and untreated hearts, fixed with 4% paraformaldehyde, and stained in suspension. The average volumes of myocytes were measured by 3D optical sectioning by confocal microscopy (16).

Nuclear DNA Content in New Myocytes and *in Situ* Hybridization. Myocytes and lymphocytes were stained with Ki67 to measure propidium iodide (PI) fluorescence intensity by confocal microscopy in noncycling and cycling EGFP^{POS} myocyte nuclei. For the detection of chromosome 12, sections were exposed to a denaturating solution containing 70% formamide. After dehydration with ethanol, sections were hybridized with rat chromosome 12/Y paint probe (Cambio, Cambridge, U.K.) for 3 h (7, 17). Nuclei were stained with PI.

Statistical Analysis. Data are reported as means ± SEM. Pairwise comparisons were performed with unpaired or paired Student's *t* tests, as appropriate. Multigroup comparisons were performed with one- or two-way (time and group) ANOVA, as appropriate, followed by Student's *t* tests with Bonferroni correction.

Results

Exclusions and Infarct Size. A total of 68 rats with infarction (32 untreated and 36 treated) and 12 sham-operated controls were studied. Eleven untreated and 10 treated rats died of ventricular fibrillation, aortic rupture, or bleeding. Four untreated and two treated rats were excluded due to failure of the coronary occluder, leaving a total of 17 untreated and 24 treated rats. Infarct size, measured as the fraction of scarred LV myocardium (18), was similar in the two groups (12.4 ± 1.7% in untreated and 13.4 ± 1.9% in treated rats). However, this method did not enable us to evaluate the effects of CSCs on infarct size, because the areas of tissue reconstitution were distributed throughout the scar. Thus, the size of the infarct and the extent of myocardial regeneration were measured by a more sophisticated quantitative method based on the number of myocytes lost and formed in the LV, respectively (see below; Fig. 6, which is published as supporting information on the PNAS web site).

Intravascular Delivery of CSCs Halts LV Remodeling and Improves LV Function. At baseline (before coronary occlusion or sham operation), echocardiographic parameters of ventricular performance were similar in untreated and CSC-treated rats. At 2 days after reperfusion, the impairment of LV systolic function, the dilation of the LV chamber, and the thinning of the LV wall were also comparable (Fig. 1; see also Fig. 7 *A–D*, which is published as supporting information on the PNAS web site), indicating that the severity of the ischemic insult was similar in the two groups.

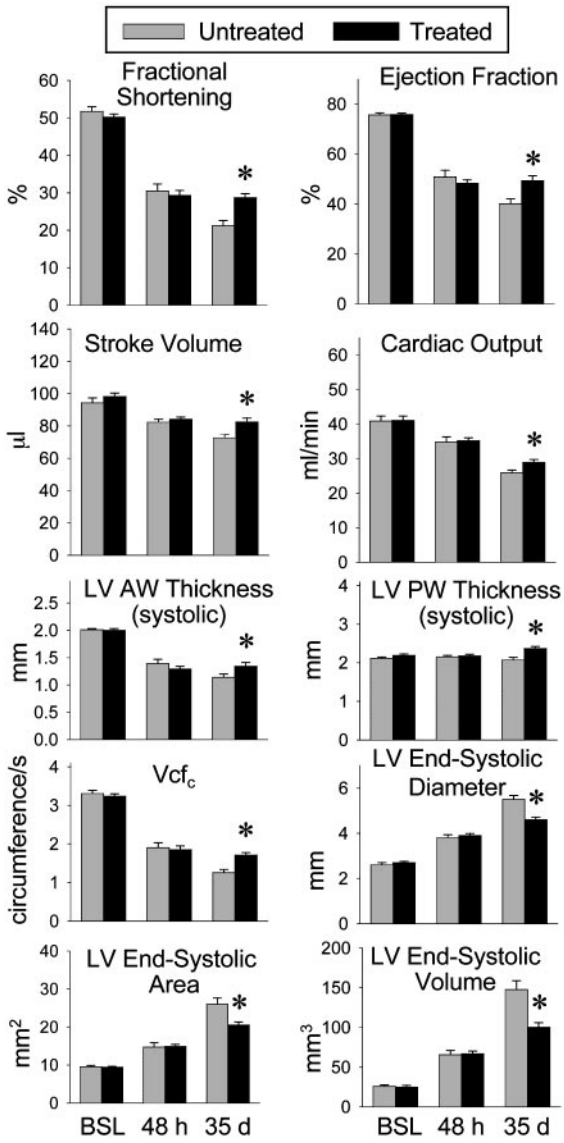

Fig. 1. Administration of CSCs improves LV systolic function. Illustrated are echocardiographic measurements in untreated and treated animals. *, $P < 0.05$ between untreated and treated rats. Data are mean ± SEM.

In untreated rats, there was further deterioration of LV systolic function, additional LV dilation, and a further decrease in LV wall thickness from 2 to 35 days after infarction, consistent with progressive LV remodeling (Figs. 1 and 7 *A–D*; see also Fig. 8, which is published as supporting information on the PNAS web site). In contrast, in rats injected with CSCs, cardiac performance, and anatomy remained essentially unchanged from 2 to 35 days. As a consequence, at 35 days after infarction, CSC-treated rats exhibited a significantly ($P < 0.01$) higher fractional shortening, ejection fraction, stroke volume, cardiac output, velocity of circumferential fiber shortening, and LV systolic wall thickness in both the infarcted and the noninfarcted regions (Figs. 1, 7 *A–D*, and 8). At the same time, CSC-treated rats had a significantly ($P < 0.01$) lower LV end-systolic diam-

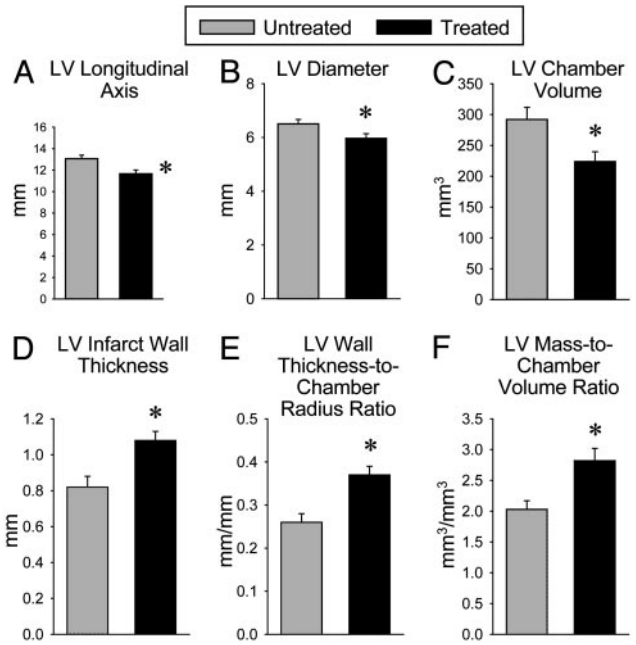

Fig. 2. Administration of CSCs improves postinfarction ventricular remodeling. Illustrated are multiple anatomical parameters obtained in hearts arrested in diastole. *, $P < 0.05$ between untreated and treated rats. Data are mean ± SEM.

eter, area, and volume compared with untreated rats (Figs. 1, 7 *A–D*, and 8). At 35 days after infarction, LV end-diastolic pressure (LVEDP) was similar in CSC-treated and untreated animals (5.6 ± 0.4 and 5.6 ± 0.9 mmHg, respectively; 1 mmHg = 133 Pa). The low values of LVEDP in infarcted animals reflect the relatively small infarcts obtained with the ischemia/reperfusion protocol used here (19).

The echocardiographic results were corroborated by the anatomical analysis of ventricular size and shape conducted in the diastolically arrested perfusion-fixed heart. In comparison with untreated animals, treated rats exhibited a smaller LV longitudinal axis, transverse chamber diameter, and chamber volume ($P < 0.01$) (Fig. 2 *A–C*). Moreover, the wall thickness-to-chamber radius ratio and the LV mass-to-chamber volume ratio were significantly ($P < 0.01$) higher in treated than in untreated rats, respectively (Fig. 2 *E* and *F*). Treated rats exhibited also a 32% ($P < 0.003$) increase in infarct wall thickness relative to untreated animals (Fig. 2*D*).

Intravascular Delivery of CSCs Promotes Myocyte Regeneration. The injection of EGFP-labeled CSCs into the aortic root led to the distribution of these cells in both the right and the left coronary circulation. A few scattered $EGFP^{POS}$ myocytes were identified in the right ventricular myocardium. Occasionally, endothelial cells and smooth muscle cells expressing EGFP were detected in the wall of small resistance arterioles and capillaries. The total number of $EGFP^{POS}$ cells in six to eight transverse sections taken 1–1.5 mm apart, spanning the entire right ventricle, varied from four to eight (Fig. 9, which is published as supporting information on the PNAS web site). These observations indicate that in the absence of tissue injury, the homing of CSCs to the myocardium was extremely limited. This was not the case in the infarcted LV.

In all treated rats subjected to infarction, $EGFP^{POS}$ cells were found both in the infarcted region (Fig. 3 *A* and *B*; see also Fig. 10, which is published as supporting information on the PNAS web site) and in the noninfarcted myocardium (posterior LV wall and septum). Myocytes were recognized by the expression of GATA-4 and MEF2C in nuclei and specific contractile proteins in the cytoplasm (Fig. 3*C*; see also Fig. 11, which is published as supporting information on the PNAS web site). Connexin 43 and N-cadherin were identified (Fig. 3*D*; see also Fig. 12, which is published as supporting information on the PNAS web site). The dual distribution of $EGFP^{POS}$ cells both within the infarct and within the surviving myocardium was not surprising, because coronary occlusion typically results in a segmental loss of myocardium in the ischemic region and in scattered apoptotic and necrotic cell death in the nonischemic region (20, 21).

In the noninfarcted LV myocardium of CSC-treated rats, regenerated $EGFP^{POS}$ myocytes constituted 0.83 ± 0.26% of myocytes. The newly formed myocytes were indistinguishable from the preexisting adjacent cells (Fig. 3*E*), suggesting that the commitment, differentiation, and maturation of CSCs into myocytes were complete by 35 days. In the infarcted region, however, the phenotype and organization of $EGFP^{POS}$ myocytes differed strikingly from those of $EGFP^{POS}$ myocytes situated in the distant noninfarcted myocardium. In contrast to the random distribution of $EGFP^{POS}$ myocytes remote from the infarct, in the infarct, the regenerated myocytes were clustered together in foci varying from 500 to 10^6 μm^2, surrounded by scarred tissue composed of collagen types III and I. Myocytes were small (970 ± 72 μm^3) and resembled neonatal cells (20), whereas the new myocytes in the noninfarcted remote myocardium were fully differentiated, possessed adult characteristics, and had a volume of 17,100 ± 1,230 μm^3 (Fig. 13, which is published as supporting information on the PNAS web site). In the noninfarcted region of treated hearts, the volume of the neighboring older $EGFP^{NEG}$ myocytes (24,500 ± 1,320 μm^3) was 43% larger ($P < 0.001$) than that of the younger $EGFP^{POS}$ cells in the same heart (Fig. 13) but was 20% smaller ($P < 0.02$) than that of the $EGFP^{NEG}$ myocytes in untreated hearts (29,500 ± 1,610 μm^3; Fig. 13), indicating that myocardial regeneration attenuated the hypertrophic response of the surviving myocytes after infarction. In comparison with myocytes in sham-operated control rats (19,000 ± 1,010 μm^3), $EGFP^{NEG}$ myocytes in CSC-treated and untreated infarcted hearts underwent 29% ($P < 0.002$) and 55% ($P < 0.001$) cellular hypertrophy after infarction, respectively.

Intravascular Delivery of CSCs Regenerates Coronary Vessels. The formation of $EGFP^{POS}$ myocytes was accompanied by the differentiation of $EGFP^{POS}$ CSCs into Ets-1^{POS}, vWF^{POS} endothelial cells and GATA-6^{POS}, α-smooth muscle $actin^{POS}$ vascular smooth muscle cells organized in new coronary arterioles and capillary structures (Figs. 14 and 15, which are published as supporting information on the PNAS web site). These newly formed coronary vessels had a thick wall and a small lumen, at times containing red blood cells. The presence of erythrocytes indicates that these coronary structures had reached functional competence and participated in the oxygenation of the reconstituted myocardium. These new vessels were distributed not only in the repairing infarct but also in the distant spared myocardium (Fig. 15 *B* and *C*). Vessel growth resulted in the formation of 134 ± 12 and 31 ± 5 $EGFP^{POS}$ capillaries per mm^2 of infarcted and viable myocardium, respectively. The corresponding numbers for $EGFP^{POS}$ arterioles were 15.2 ± 1.8 and 0.5 ± 0.1 per mm^2. Individual $EGFP^{POS}$ endothelial and smooth muscle cells distributed irregularly in vascular structures were also identified in the nonischemic LV myocardium of CSC-treated infarcted rats.

Intravascular Delivery of CSCs Reduces Infarct Size. The total number of myocytes lost and remaining in the ventricle after MI provides a reliable assessment of the magnitude of the insult and of the degree of cardiac recovery at 35 days (16). The percentage of myocytes lost in treated and untreated hearts was 27%

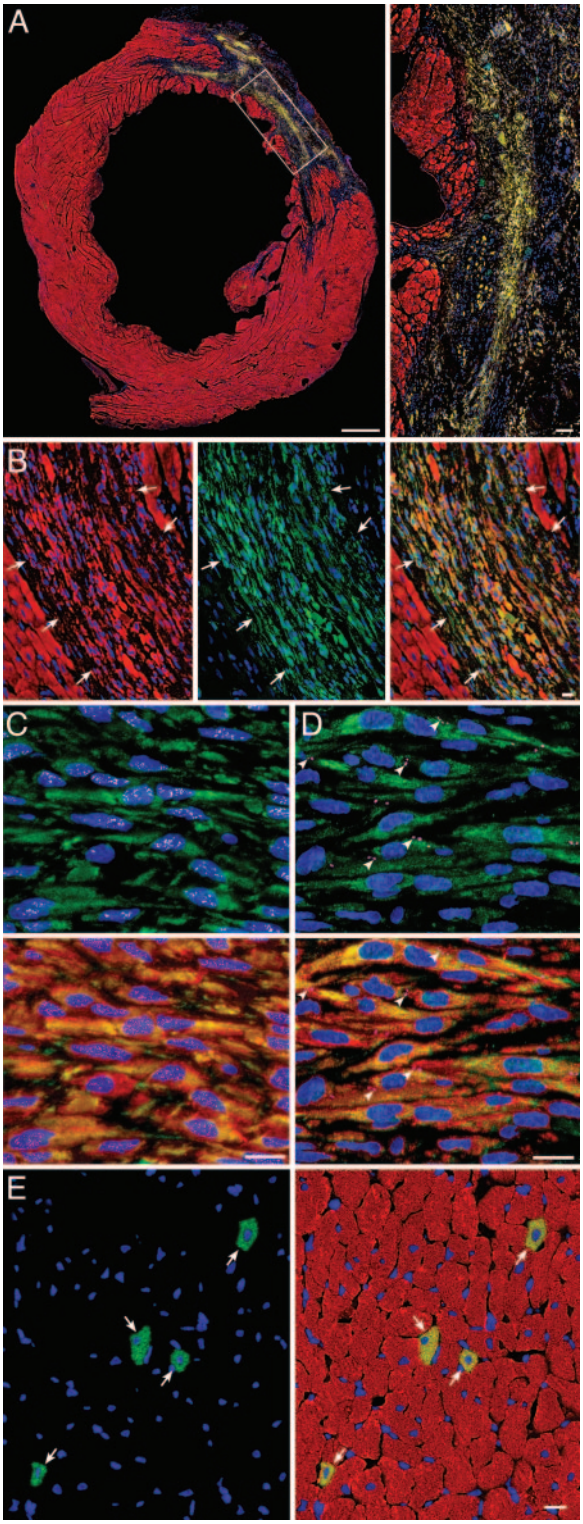

Fig. 3. Administration of CSCs promotes myocardial regeneration. (*A*) Large transverse section halfway between the base and the apex of the left ventricle, showing an infarct in a CSC-treated rat. (*Inset*) Regenerated infarcted myocardium (EGFP and α-sarcomeric actin, yellow-green). (Bars, 1 mm and 100 μm.) (*B*) Another example of regenerated infarcted myocardium (arrows) is shown first by α-sarcomeric actin staining (red), then by EGFP labeling (green) and then by the combination of EGFP and α-sarcomeric actin (yellow-green). (*C*) EGFP^{POS} (green), α-sarcomeric actin^{POS} (red), small newly formed myocytes within the infarcted region express in their nuclei GATA-4 (white) and MEF2C (magenta). (*D*) EGFP^{POS} (green), cardiac myosin heavy chain^{POS} (red) small newly formed myocytes within the infarcted region express in their plasma membrane connexin 43 (magenta, arrowheads). (*E*) Newly formed myocytes in the surviving noninfarcted LV myocardium (arrows) are shown first by EGFP labeling (green) and then by the combination of EGFP and α-sarcomeric actin (yellow-green) [Bar (*B–E*), 10 μm.]

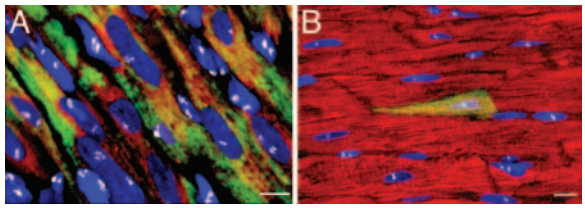

Fig. 4. Administration of CSCs promotes regeneration in the absence of cell fusion. (*A* and *B*) Nuclear localization of chromosome 12 (white dots) is shown in newly formed EGFP^{POS}-α-sarcomeric actin^{POS} (yellow-green) myocytes in the infarcted (*A*) and spared (*B*) myocardium.

(-6.0×10^6 myocytes) and 33% (-7.2×10^6 myocytes), respectively (Fig. 6). In the treated group, this value reflects the size of the original infarct, because the contribution of EGFP^{POS} myocytes was not included in these measurements (this was done to assess infarct size independently of the myocyte regeneration associated with the injection of CSCs). Because the regenerated myocardium replaced 18.8 ± 2.8% of the scarred infarct and was composed of 16.6×10^6 EGFP^{POS} myocytes, over a period of 35 days, CSCs formed 3-fold more myocytes than those originally lost (5.9×10^6 myocytes). The reconstituted myocardium, however, replaced only 18.1 mm^3 of the 78.9 mm^3 of tissue lost by ischemic injury (Fig. 6). Therefore, the repair process regenerated an excess of myocytes but fell short in tissue reconstitution. This was due to the failure of new myocytes to reach the adult phenotype. An additional component of myocardial regeneration was the formation of new myocytes scattered throughout the spared myocardium. This type of repair included 0.2×10^6 EGFP^{POS} myocytes with an aggregate myocyte volume of 3.5 mm^3 and a total myocardial volume of 4.6 mm^3. Altogether, 22.7 mm^3 of tissue was reconstituted, and infarct size was decreased by 29%, from a loss of 78.9 mm^3 of myocardium in untreated hearts to a loss of 56.2 mm^3 of tissue in CSC-treated hearts. Each morphometric step implicated in this complex analysis of infarct size and myocardial restoration is illustrated in Fig. 6. It should be noted that the numbers obtained with these methods are estimates (16).

Intravascular Delivery of CSCs Does Not Result in Cell Fusion. To establish whether cell fusion contributed to myocardial regeneration, DNA content was measured in nuclei of isolated EGFP^{POS} myocytes, and the number of chromosomes 12 was assessed in tissue sections. CSC-derived myocytes had nuclei with 2C DNA content (Fig. 16, which is published as supporting information on the PNAS web site). Cycling Ki67^{POS} myocytes and lymphocytes had a DNA content intermediate between diploid and tetraploid (Fig. 16*B*). Importantly, in all cases, only two chromosomes 12 were detected in newly formed EGFP^{POS} myocytes (Fig. 4 *A* and *B*). Thus, the administration of CSCs led to myocardial regeneration that was largely independent of cell fusion.

In the region bordering the infarct, the percentage of Ki67^{POS}, EGFP^{NEG} myocytes was similar in untreated and CSC-treated hearts (0.45 ± 0.13% and 0.48 ± 0.18%, respectively (Table 2, which is published as supporting information on the PNAS web site). Similarly, the length density of capillaries in the border zone was similar in untreated and CSC-treated hearts (3,152 ± 489 mm/mm^3 and 3,312 ± 541 mm/mm^3, respectively) (Table 2). These data suggest that the injected CSCs did not exert a

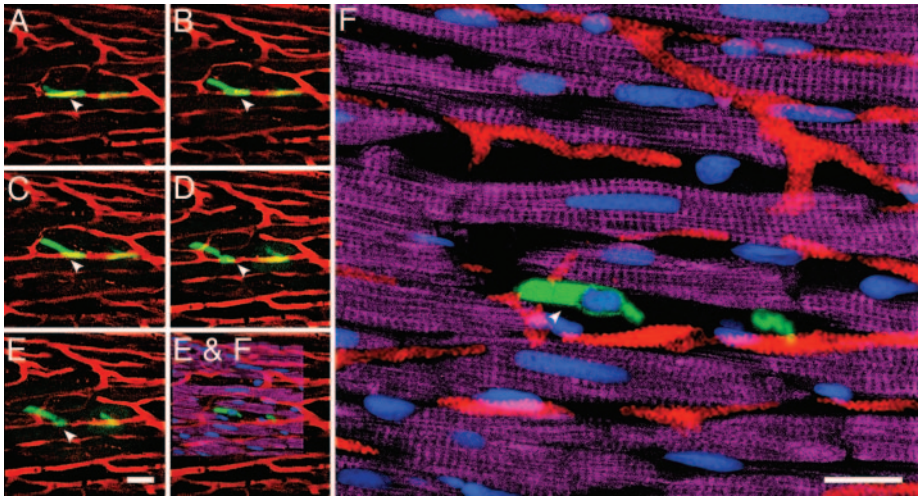

Fig. 5. CSCs traverse the wall of coronary vessels migrating to the myocardium. (*A*) Detection by two-photon microscopy of numerous EGFP^{POS} clonogenic CSCs (green) located within the lumen of coronary vessels (rhodamine-labeled dextran; red) 20 min after cell injection. (*A–E*) Transcoronary migration of EGFP^{POS} CSCs to the myocardium; images of the same field (*A–E*) were taken at 30-min intervals, starting at 30 min after the intravascular delivery of these cells. Arrowheads point to the cells that translocated through the vessel wall (*C–E*). Arrowheads point to the same EGFP^{POS} CSCs detected in the living tissue by two-photon microscopy (*E*, green) and after fixation, embedding, and staining of the same region of the ventricular wall by confocal microscopy (*F*, green). Myocytes are stained by cardiac myosin (magenta), and nuclei are labeled by DAPI (blue). Red fluorescence in the confocal microscopic image illustrates the coronary circulation (rhodamine-labeled dextran, red). (*Inset*) Superimposition of *E* and *F*. Two-photon microscopy: focal depth, 20 μm. Confocal microscopy: section thickness, 10 μm. (Bars, 20 μm.)

paracrine effect that promoted the growth of spared myocytes or vascular growth in the surviving myocardium. Interestingly, in treated hearts, a significant fraction of EGFP^{POS} myocyte nuclei were Ki67^{POS} (Fig. 17, which is published as supporting information on the PNAS web site, and Table 2), indicating that at 5 weeks after infarction, these CSC-derived myocytes have not reached terminal differentiation and growth arrest but rather possess a residual capacity to divide.

Transcoronary Migration of EGFP^{POS} CSCs. To obtain direct evidence for the ability of CSCs to cross the wall of coronary vessels and reach the damaged myocardium, rats subjected to a 90-min coronary occlusion followed by reperfusion were injected with EGFP^{POS} CSCs. The locomotion of CSCs was then assessed *ex vivo* by two-photon microscopy after perfusion of the coronary vasculature with rhodamine-labeled dextran (Fig. 5; see also Fig. 18, which is published as supporting information on the PNAS web site). The tissue was then fixed with formalin and detailed analysis performed by immunostaining and confocal microscopy. At 4 h after reperfusion and 20 min after CSC delivery, a large number of EGFP^{POS} cells were identified within the coronary vasculature (Fig. 18*A*). EGFP^{POS} cells migrated across the wall of the vessels and within 3 h moved into the ischemic area (Fig. 5). At 12 h after reperfusion and 8 h after the injection of CSCs, EGFP^{POS} cells were detected in groups within areas of myocardium with disrupted vessels and diffuse distribution of fluorescent dextran (Fig. 18*B*). Thus, intraarterial delivery of CSCs led to their extravasation and homing to the interstitial compartment of the heart within a few hours. Immunoblotting analysis of CSCs demonstrated expression of CXCR4 in these cells (Fig. 19, which is published as supporting information on the PNAS web site). This finding, coupled with the previous finding that SDF-1 is up-regulated in the ischemic reperfused myocardium (22), suggests that the SDF-1/CXCR4 axis plays a role in the homing of CSCs to the injured tissue.

Discussion

The postnatal heart is commonly thought to be a terminally differentiated postmitotic organ. However, this view has recently been refuted by the finding that the adult heart harbors primitive cells that exhibit both the markers and the phenotype of multipotent stem/progenitor cells (8–12). We hypothesized that adult CSCs would serve as the most suitable substrate for cardiac regeneration. Although hematopoietic stem cells, skeletal myoblasts, neonatal myocytes, and mesenchymal and embryonic stem cells have all been used, each of these approaches has shown limitations (1, 23, 24).

The salient results of the present study can be summarized as follows: (*i*) CSCs injected into the coronary circulation are able to cross the vessel wall and enter the interstitium of the heart within few hours; (*ii*) intravascular administration of CSCs produces quantitatively important tissue regeneration that comprises cardiomyocytes and vascular structures (endothelial and smooth muscle cells), resulting in restoration of the number of myocytes in the infarcted region; (*iii*) this anatomical reconstitution is associated with beneficial effects on LV remodeling and dysfunction, including attenuation of LV chamber dilation and wall thinning and improvement of systolic performance; (*iv*) CSCs give rise to new myocytes both in the infarcted and noninfarcted regions, although the phenotype of the cells differs in the two settings; (*v*) the formation of EGFP^{POS} myocytes is not due to cell fusion and therefore reflects differentiation of CSCs into new myocytes; and (*vi*) CSCs do not appear to promote growth of surviving cells via paracrine effects. Importantly, the beneficial effects of CSCs were observed in the setting of transient ischemia followed by reperfusion, which is relevant to the majority of patients with MI, and using a route of CSC administration that is easily accessible in patients.

Previous studies have documented the ability of CSCs to regenerate infarcted myocardium when injected intramyocardially in the periinfarct region after a permanent coronary occlusion (9, 12). A very modest degree of regeneration has also been reported after i.v. injection of CSCs (10). The present study reveals several fundamental aspects of CSC-mediated cardiac repair that have not been previously described, namely, (*i*) CSCs effectively repair infarcted myocardium in the presence of coronary reperfusion, (*ii*) CSCs are effective when given intravascularly, (*iii*) the cardiac regeneration effected by intravascular

CSCs results in important cardiac functional changes, and (*iv*) the salubrious effects of CSCs are not due to cell fusion.

The recognition that CSCs can differentiate into two cell populations (small poorly differentiated myocytes and large myocytes with adult characteristics) is one of the most interesting findings of this study. The small myocytes reside in the infarcted region (Figs. 3 *A* and *B* and 10), whereas the large ones are located in the periinfarct territory and in the distant myocardium (Figs. 3*E* and 9). Although the factors that govern the differentiation of CSCs into small vs. large parenchymal cells remain unknown, it seems reasonable to postulate that contact with mature myocytes and paracrine factors may play a role in determining the final size of the cells after lineage commitment of CSCs.

The present observations also provide insights into the mechanism whereby CSCs reconstitute dead myocardial tissue. Although fusion of bone marrow cells with resident parenchymal cells of the target organ has been documented in other systems (25–29), this phenomenon cannot account for the beneficial effects of CSCs observed in the present study, because all $EGFP^{POS}$ cells were found to be diploid using two independent methods. Furthermore, the similarity in the number of $EGFP^{NEG}$ $Ki67^{POS}$ myocytes and in capillary density between control and CSC-treated hearts suggests that CSCs did not exert a paracrine growth-promoting effect on the surviving cardiac cells. Collectively, our results indicate that intravascular CSCs home to the infarcted heart where they commit themselves to the cardiac cell lineages, replacing dead myocardium. In this study, CSCs were assessed by comparing them with vehicle. We did not examine the physiological effects or the regenerative capacity of a control cell population (i.e., a population of nonprogenitor cells).

Our findings have obvious translational implications for the treatment of patients with acute MI and ischemic cardiomyopathy. Although the CSCs used here were obtained from syngeneic donors, in the clinical arena, autologous CSCs could be isolated from small myocardial biopsies, expanded *in vitro*, and subsequently administered to the same patient. Preliminary results support the feasibility of this approach (R.B. and P.A., unpublished data). Prophylactic harvesting of CSCs followed by cryopreservation would ensure that adequate numbers of cells are readily available if and when the patient suffers an acute MI.

Conclusion

This study reveals that CSCs are effective when delivered in a clinically relevant manner, a clear prerequisite for clinical translation, and that the mechanism for their beneficial effects is independent of cell fusion. The results reported herein establish CSCs as candidates for cardiac regeneration and support a novel approach in which the heart's own stem cells could be collected, expanded, and stored for subsequent therapeutic repair.

We are grateful to Stefano Chimenti for expert technical assistance. This work was supported in part by National Institutes of Health Grants R01 HL-55757, HL-68088, HL-70897, HL-76794, HL-72410, HL-38132, HL-39902, AG-15756, HL-66923, HL-65573, HL-65577, AG-17042, and AG-023071.

1. Rosenthal, N. (2003) *N. Engl. J. Med.* **349,** 267–274.
2. Strauer, B. E., Brehm, M., Zeus, T., Kostering, M., Hernandez, A., Sorg, R. V., Kogler, G. & Wernet, P. (2002) *Circulation* **106,** 1913–1918.
3. Britten, M. B., Abolmaali, N. D., Assmus, B., Lehmann, R., Honold, J., Schmitt, J., Vogl, T. J., Martin, H., Schachinger, V., Dimmeler, S., *et al.* (2003) *Circulation* **108,** 2212–2218.
4. Perin, E. C., Dohmann, H. F., Borojevic, R., Silva, S. A., Sousa, A. L., Mesquita, C. T., Rossi, M. I., Carvalho, A. C., Dutra, H. S., Dohmann, H. J., *et al.* (2003) *Circulation* **107,** 2294–2302.
5. Stamm, C., Westphal, B., Kleine, H. D., Petzsch, M., Kittner, C., Klinge, H., Schumichen, C., Nienaber, C. A., Freund, M. & Steinhoff, G. (2003) *Lancet* **361,** 45–46.
6. Tse, H. F., Kwong, Y. L., Chan, J. K., Lo, G., Ho, C. L. & Lau, C. P. (2003) *Lancet* **361,** 47–49.
7. Quaini, F., Urbanek, K., Beltrami, A. P., Finato, N., Beltrami, C. A., Nadal-Ginard, B., Kajstura, J., Leri, A. & Anversa, P. (2002) *N. Engl. J. Med.* **346,** 5–15.
8. Urbanek, K., Quaini, F., Tasca, G., Torella, D., Castaldo, C., Nadal-Ginard, B., Leri, A., Kajstura, J., Quaini, E. & Anversa, P. (2003) *Proc. Natl. Acad. Sci. USA* **100,** 10440–10445.
9. Beltrami, A. P., Barlucchi, L., Torella, D., Baker, M., Limana, F., Chimenti, S., Kasahara, H., Rota, M., Musso, E., Urbanek, K., *et al.* (2003) *Cell* **114,** 763–776.
10. Oh, H., Bradfute, S. B., Gallardo, T. D., Nakamura, T., Gaussin, V., Mishina, Y., Pocius, J., Michael, L. H., Behringer, R. R., Garry, D. J., *et al.* (2003) *Proc. Natl. Acad. Sci. USA* **100,** 12313–12318.
11. Matsuura, K., Nagai, T., Nishigaki, N., Oyama, T., Nishi, J., Wada, H., Sano, M., Toko, H., Akazawa, H., Sato, T., *et al.* (2004) *J. Biol. Chem.* **279,** 11384–11391.
12. Messina, E., De Angelis, L., Frati, G., Morrone, S., Chimenti, S., Fiordaliso, F., Salio, M., Battaglia, M., Latronico, M. V., Coletta, M., *et al.* (2004) *Circ. Res.* **95,** 911–921.
13. Bolli, R., Becker, L., Gross, G., Mentzer, R. J., Balshaw, D. & Lathrop, D. A. (2004) *Circ. Res.* **95,** 125–134.
14. Kloner, R. A. & Jennings, R. B. (2001) *Circulation* **104,** 2981–2989.
15. Pawlush, D. G., Moore, R. L., Musch, T. I. & Davidson, W. R., Jr. (1993) *J. Appl. Physiol.* **74,** 2598–2605.
16. Anversa, P. & Olivetti, G. (2002) in *The Heart*, eds. Page, E., Fozzard, H. A. & Solaro, R. J. (Oxford Univ. Press, New York), **Vol. I,** pp. 75–144.
17. Orlic, D., Kajstura, J., Chimenti, S., Jakoniuk, I., Anderson, S. M., Li, B., Pickel, J., McKay, R., Nadal-Ginard, B., Bodine, D. M., *et al.* (2001) *Nature* **410,** 701–705.
18. Li, Q., Li, B., Wang, X., Leri, A., Jana, K. P., Liu, Y., Kajstura, J., Baserga, R. & Anversa, P. (1997) *J. Clin. Invest.* **100,** 1991–1999.
19. Pfeffer, M. A., Pfeffer, J. M., Fishbein, M. C., Fletcher, P. J., Spadaro, J., Kloner, R. A. & Braunwald, E. (1979) *Circ. Res.* **44,** 503–512.
20. Anversa, P. & Nadal-Ginard, B. (2002) *Nature* **415,** 240–243.
21. Nadal-Ginard, B., Kajstura, J., Leri, A. & Anversa, P. (2003) *Circ. Res.* **92,** 139–150.
22. Kucia, M., Dawn, B., Hunt, G., Guo, Y., Wysoczynski, M., Majka, M., Ratajczak, J., Rezzoug, F., Ildstad, S. T., Bolli, R., *et al.* (2004) *Circ. Res.* **95,** 1191–1199.
23. Torella, D., Rota, M., Nurzynska, D., Musso, E., Monsen, A., Shiraishi, I., Zias, E., Walsh, K., Rosenzweig, A., Sussman, M. A., *et al.* (2004) *Circ. Res.* **94,** 514–524.
24. Leri, A., Kajstura, J., Nadal-Ginard, B. & Anversa, P. (2004) *Circ. Res.* **94,** 132–134.
25. Alvarez-Dolado, M., Pardal, R., Garcia-Verdugo, J. M., Fike, J. R., Lee, H. O., Pfeffer, K., Lois, C., Morrison, S. J. & Alvarez-Buylla, A. (2003) *Nature* **425,** 968–973.
26. Corbel, S. Y., Lee, A., Yi, L., Duenas, J., Brazelton, T. R., Blau, H. M. & Rossi, F. M. (2003) *Nat. Med.* **9,** 1528–1532.
27. Vassilopoulos, G., Wang, P. R. & Russell, D. W. (2003) *Nature* **422,** 901–904.
28. Wang, X., Willenbring, H., Akkari, Y., Torimaru, Y., Foster, M., Al-Dhalimy, M., Lagasse, E., Finegold, M., Olson, S. & Grompe, M. (2003) *Nature* **422,** 897–901.
29. Weimann, J. M., Charlton, C. A., Brazelton, T. R., Hackman, R. C. & Blau, H. M. (2003) *Proc. Natl. Acad. Sci. USA* **100,** 2088–2093.